Detrending-moving-average-based bivariate regression estimator

Qingju Fan
Department of Statistics, School of Science, Wuhan University of Technology, Wuhan 430070, People's Republic of China

Fang Wang*
College of Information and Telligence/Agricultural Mathematical Modeling and Data Processing Center, Hunan Agricultural University, Changsha 410128, People's Republic of China

(Received 19 March 2020; revised 29 May 2020; accepted 4 July 2020; published 24 July 2020)

In this work, a detrending-moving-average- (DMA) based bivariate linear regression analysis method is proposed. The method is combination of detrended moving average analysis and standard regression methodology, which allows us to estimate the scale-dependent regression coefficients for nonstationary and power-law correlated time series. By using synthetic simulations with error of estimation for different position parameter θ of detrending windows, we test our DMA-based bivariate linear regression algorithm and find that the centered detrending technique ($\theta = 0.5$) is of best performance, which provides the most accurate estimates. In addition, the estimated regression coefficients are in good agreement with the theoretical values. The center DMA-based bivariate linear regression estimator is applied to analyze the return series of Shanghai stock exchange composite index, the Hong Kong Hangseng index and the NIKKEI 225 index. The dependence among the Asian stock market across timescales is confirmed. Furthermore, two statistics based on the scale-dependent t statistic and the partial detrending-moving-average cross-correlation coefficient are used to demonstrate the significance of the dependence. The scale-dependent evaluation parameters also show that the DMA-based bivariate regression model can provide rich information than standard regression analysis.

DOI: 10.1103/PhysRevE.102.012218

I. INTRODUCTION

Detrended fluctuation analysis (DFA) is one of the most popular and reliable method in fractal analysis [1,2] which can explore the long-range autocorrelations and multifractal features of time series in diverse fields [3–11]. Alternatively, the detrending-moving-average (DMA) method and its generalized various versions can also be used for multifractal analysis [12–21]. Synthetic tests suggest that the performance of the DMA method is comparable to the DFA method with slightly different priorities under certain circumstances [22–24]. Furthermore, the competitive methods have similar performances while the DMA algorithms are computationally less demanding as they contain no box splitting and regression fitting in most cases [25,26].

Recently, DFA- and DMA-based regression analysis method for bivariate series have been developed to analyze the nonstationary and long-range-dependent data at different scales [27,28]. The DFA-based regression method [27] is based on the least-squares estimator, translated by the scale-dependent detrended fluctuation variance and covariance which is obtained by DFA and detrended cross correlation analysis (DCCA) [29]. The DFA-DCCA setting is capable of estimating regression parameters, standard errors of the estimates, and the coefficient of determination for specific scales. Similarly, DMA-based regression framework was also formulated [28]. The most important advantage of DFA- or DMA-based regression estimators over standard linear regression analysis is the interpretation of the dependence between two variables at different time periods. Furthermore, DFA-based bivariate regression model was introduced to investigate the dependence among PM2.5 series of three adjacent cities [30].

In this work, we propose an alternative but also a complementary estimators DMA-based bivariate regression model, which is constructed by merging standard regression least squares with detrending-moving-average analysis. The framework not only allows for studying the dependence among variables at different scales but also provides related standard errors and coefficients of determination. Since the DMA algorithm is comparable to the DFA algorithm, we expect that the DMA-based bivariate regression model will show similar advantages. Our numerical experiments and empirical analysis confirm this conjecture.

The rest is organized as follows: In Sec. II, we briefly recall standard bivariate regression analysis and introduce the DMA-based bivariate regression model. In Sec. III, first, we conduct the numerical simulation to test the validity of the proposed method and present comparing results with DFA-based bivariate regression model; then we discuss the financial series used to develop our method, including regression parameter estimates, statistical significance test, and discussion of the coefficient of determination, etc. This study represent a point of view of a practitioner who wants to choose a better tool for his or her analyses without entering

*Corresponding author: popwang619@163.com

subtle theoretical considerations. Section IV gives a brief summary.

II. METHODOLOGY

A. The standard bivariate regression model

The bivariate linear regression model is designed to study the dependence among series, described as

$$Z = \beta_0 + \beta_1 X + \beta_2 Y + \epsilon, \tag{1}$$

where Z is a dependent (response) variable, X and Y are two independent (impulse) variables, ϵ is a Gaussian error term with zero mean value, and β_1 and β_2 are the partial regression coefficients characterizing the dependence on X and Y, respectively. The next key point for researchers is to estimate β_1 and β_2 in empirical studies. The ordinary least-squares (OLS) method is utilized by

$$\begin{aligned}\hat{\beta}_1 &= \frac{\left(\sum_{t=1}^N x_t z_t\right)\left(\sum_{t=1}^N y_t^2\right) - \left(\sum_{t=1}^N y_t z_t\right)\left(\sum_{t=1}^N x_t y_t\right)}{\left(\sum_{t=1}^N x_t^2\right)\left(\sum_{t=1}^N y_t^2\right) - \left(\sum_{t=1}^N x_t y_t\right)^2}, \\ &\sim \frac{\widehat{\sigma_{XZ}}\widehat{\sigma_Y^2} - \widehat{\sigma_{YZ}}\widehat{\sigma_{XY}}}{\widehat{\sigma_X^2}\widehat{\sigma_Y^2} - \widehat{\sigma_{XY}}^2},\end{aligned} \tag{2}$$

$$\begin{aligned}\hat{\beta}_2 &= \frac{\left(\sum_{t=1}^N y_t z_t\right)\left(\sum_{t=1}^N x_t^2\right) - \left(\sum_{t=1}^N x_t z_t\right)\left(\sum_{t=1}^N x_t y_t\right)}{\left(\sum_{t=1}^N x_t^2\right)\left(\sum_{t=1}^N y_t^2\right) - \left(\sum_{t=1}^N x_t y_t\right)^2}, \\ &\sim \frac{\widehat{\sigma_{YZ}}\widehat{\sigma_X^2} - \widehat{\sigma_{XZ}}\widehat{\sigma_{XY}}}{\widehat{\sigma_X^2}\widehat{\sigma_Y^2} - \widehat{\sigma_{XY}}^2}.\end{aligned} \tag{3}$$

where $x_t = X_t - \langle X_t \rangle$, $y_t = Y_t - \langle Y_t \rangle$, and $z_t = Z_t - \langle Z_t \rangle$ and $\langle \cdot \rangle$ denotes the mean value. By using the residuals $\hat{e}_t = Z_t - \hat{\beta}_1 X_t - \hat{\beta}_2 Y_t - \langle Z_t - \hat{\beta}_1 X_t - \hat{\beta}_2 Y_t \rangle$, variance of the estimator of residuals is obtained by

$$\begin{aligned}\mathrm{var}(\hat{\beta}_1) &= \frac{\left(\sum_{t=1}^N y_t^2\right)\frac{\sum_{t=1}^N \hat{e}_t{}^2}{N-3}}{\left(\sum_{t=1}^N x_t^2\right)\left(\sum_{t=1}^N y_t^2\right) - \left(\sum_{t=1}^N x_t y_t\right)^2} \\ &\sim \frac{1}{N-3}\frac{\widehat{\sigma_Y}\widehat{\sigma_\epsilon^2}}{\widehat{\sigma_X^2}\widehat{\sigma_Y^2} - \widehat{\sigma_{XY}}^2},\end{aligned} \tag{4}$$

$$\begin{aligned}\mathrm{var}(\hat{\beta}_2) &= \frac{\left(\sum_{t=1}^N x_t^2\right)\frac{\sum_{t=1}^N \hat{e}_t{}^2}{N-3}}{\left(\sum_{t=1}^N x_t^2\right)\left(\sum_{t=1}^N y_t^2\right) - \left(\sum_{t=1}^N x_t y_t\right)^2} \\ &\sim \frac{1}{N-3}\frac{\widehat{\sigma_X}\widehat{\sigma_\epsilon^2}}{\widehat{\sigma_X^2}\widehat{\sigma_Y^2} - \widehat{\sigma_{XY}}^2}.\end{aligned} \tag{5}$$

The variance explains the accuracy of the estimated parameters, and the estimated regression coefficients together with their corresponding variances can be further utilized for hypothesis test and model evaluation. To evaluate the efficiency of the regression model, the following determination coefficient R^2, β coefficient β^*, and elasticity coefficient η are also given by

$$R^2 = 1 - \frac{\sum_{t=1}^N \hat{e}_t{}^2}{\sum_{t=1}^N y_t^2} = 1 - \frac{\widehat{\sigma_\epsilon^2}}{\widehat{\sigma_Z^2}}, \tag{6}$$

$$\begin{cases}\beta_1^* = \hat{\beta}_1\sqrt{\frac{\sum_{t=1}^N x_t^2}{\sum_{t=1}^N z_t^2}}, \\ \beta_2^* = \hat{\beta}_2\sqrt{\frac{\sum_{t=1}^N y_t^2}{\sum_{t=1}^N z_t^2}},\end{cases} \tag{7}$$

$$\begin{cases}\eta_1 = \hat{\beta}_1\frac{\langle X\rangle}{\langle Z\rangle}, \\ \eta_2 = \hat{\beta}_2\frac{\langle Y\rangle}{\langle Z\rangle}.\end{cases} \tag{8}$$

Generally speaking, R^2 ranges in $(0, 1)$, which quantifies a proportion of variance of Z explained by X and Y, and the higher value of R^2 implies a better model explaining ability. The above $\beta_j^*(j = 1, 2)$ coefficient is described to quantify the sensitivity of explained variable to each explaining variable, and $\eta_j(j = 1, 2)$ is the average elasticity coefficient, which can explain the relative importance of variables X and Y to Z.

B. Detrended moving average and cross-correlation analysis (DMA and XDMA)

The DMA and XDMA methodology is well described in Refs. [13,16–18]. Here we briefly outline the variance and covariance procedure in the following. Suppose that $\{x_t\}$ is a time series with length N. The sequence of cumulative sums is $X(t) = \sum_{k=1}^t x_k$, for $t = 1, 2, \ldots, N$, and the moving average function in a moving window is defined as

$$\tilde{X}(t) = \frac{1}{s}\sum_{k=-\lfloor(s-1)\theta\rfloor}^{\lceil(s-1)(1-\theta)\rceil} X(t-k), \tag{9}$$

where s is the window size and θ is a factor of of moving average type ranging in $[0, 1]$ (forward, centered, and backward for $\theta = 0$, $\theta = 0.5$, and $\theta = 1$, respectively). The residual series is obtained as $\epsilon(i) = X(i) - \tilde{X}(i)$ for $s - \lfloor(s-1)\theta\rfloor \leqslant i \leqslant N - \lfloor(s-1)\theta\rfloor$, which is divided into $N_s = \lfloor N/s - 1\rfloor$ disjoint segments with the same size s. In the vth box, $\epsilon_v(i) = \epsilon((v-1)s + i)$ for $1 \leqslant i \leqslant s$ the fluctuation function can be calculated by

$$f_{XX}^2(s, v) = \frac{1}{s}\sum_{i=1}^s [X(i) - \tilde{X}(i)]^2. \tag{10}$$

Averaging the fluctuation function $f_{XX}^2(s, v)$ over all the box gets

$$F_{XX}^2(s) = \frac{1}{N_s}\sum_{v=1}^{N_s} f_{XX}^2(s, v). \tag{11}$$

In a similar way, we get the detrended covariance of bivariate series $\{x_t\}$ and $\{y_t\}$, which is determined as

$$f_{XY}^2(s, v) = \frac{1}{s}\sum_{i=1}^s [X(i) - \tilde{X}(i)][Y(i) - \tilde{Y}(i)], \tag{12}$$

$$F_{XY}^2(s) = \frac{1}{N_s}\sum_{v=1}^{N_s} f_{XY}^2(s, v). \tag{13}$$

$F_{XX}^2(s)$ and $F_{XY}^2(s)$ are considered as scale-dependent variance and covariance, respectively.

C. DMA-based bivariate regression estimator

In this section, the detrending-moving-average-based bivariate regression estimator is proposed. Motivated by the idea in Refs. [27,28,30], we utilize the correspondence of variance and covariance in Eqs. (11) and (13), and then two scale-dependent estimators translated from Eqs. (2) and (3) are obtained through

$$\begin{cases} \hat{\beta}_1^{\mathrm{DMA}}(s) & = \frac{F_{XZ}^2(s)F_Y^2(s)-F_{YZ}^2(s)F_{XY}^2(s)}{F_X^2(s)F_Y^2(s)-[F_{XY}^2(s)]^2}, \\ \hat{\beta}_2^{\mathrm{DMA}}(s) & = \frac{F_{YZ}^2(s)F_X^2(s)-F_{XZ}^2(s)F_{XY}^2(s)}{F_X^2(s)F_Y^2(s)-[F_{XY}^2(s)]^2}. \end{cases} \tag{14}$$

Similarly, the scale-dependent residuals can also be reformulated as

$$\hat{e}_t(s) = Z_t - \hat{\beta}_1^{\mathrm{DMA}} X_t - \hat{\beta}_2^{\mathrm{DMA}} Y_t - \langle Z_t - \hat{\beta}_1^{\mathrm{DMA}} X_t - \hat{\beta}_2^{\mathrm{DMA}} Y_t \rangle. \tag{15}$$

with zero mean value. Furthermore, DMA algorithm is applied to $\hat{e}_t(s)$, and the calculated fluctuation $F_\epsilon^2(s)$ can be used to estimate the variance of $\hat{\beta}_j^{\mathrm{DMA}}$ $(j = 1, 2)$ in Eq. (14),

$$\begin{cases} \mathrm{var}[\hat{\beta}_1^{\mathrm{DMA}}(s)] & = \frac{1}{N-3}\frac{F_Y^2(s)F_\epsilon^2(s)}{F_Y^2(s)-[F_{XY}^2(s)]^2}, \\ \mathrm{var}[\hat{\beta}_2^{\mathrm{DMA}}(s)] & = \frac{1}{N-3}\frac{F_X^2(s)F_\epsilon^2(s)}{F_Y^2(s)-[F_{XY}^2(s)]^2}. \end{cases} \tag{16}$$

The corresponding scale-specific determination coefficient $R_{\mathrm{DMA}}^2(s)$, β coefficient $\beta^{*\mathrm{DMA}}(s)$, and elasticity coefficient $\eta^{\mathrm{DMA}}(s)$ are presented as follows:

$$R_{\mathrm{DMA}}^2(s) = 1 - \frac{F_\epsilon^2(s)}{F_Z^2(s)}, \tag{17}$$

$$\begin{cases} \beta_1^{*\mathrm{DMA}}(s) = \hat{\beta}_1^{\mathrm{DMA}}(s)\sqrt{\frac{F_X^2(s)}{F_Z^2(s)}}, \\ \beta_2^{*\mathrm{DMA}}(s) = \hat{\beta}_2^{\mathrm{DMA}}(s)\sqrt{\frac{F_Y^2(s)}{F_Z^2(s)}}, \end{cases} \tag{18}$$

$$\begin{cases} \eta_1^{\mathrm{DMA}}(s) = \hat{\beta}_1^{\mathrm{DMA}}(s)\frac{\langle X\rangle}{\langle Z\rangle}, \\ \eta_2^{\mathrm{DMA}}(s) = \hat{\beta}_2^{\mathrm{DMA}}(s)\frac{\langle Y\rangle}{\langle Z\rangle}. \end{cases} \tag{19}$$

III. NUMERICAL EXPERIMENTS

In order to test the validity and performance of the proposed DMA-based bivariate regression estimator, we first perform two numerical experiments. It is worth noting that different position types (forward, centered, and backward for $\theta = 0$, $\theta = 0.5$, and $\theta = 1$, respectively) of moving averages schemes produce different results. Some literatures have reported that the centered one ($\theta = 0.5$) showed the best results [17,31]. For the sake of completeness, we first compare the error results of different moving averages schemes on the two simulations and then present the results of the best scheme. Artificial series are generated by autoregressive fractionally integrated moving-average process (ARFIMA (0, d, 0)) [32],

$$\begin{cases} X_t = \sum_{n=1}^{\infty} \alpha_n(d_1)\xi_1(t-n), \\ Y_t = \sum_{n=1}^{\infty} \alpha_n(d_2)\xi_2(t-n). \end{cases} \tag{20}$$

where $d_i (i = 1, 2)$ is fractional integration parameters with the range $(-0.5, 0.5)$, $\alpha_n(d_i) = \Gamma(n-d_i)/[\Gamma(-d_i)\Gamma(n+1)]$, and $\Gamma(\cdot)$ denotes the Gamma function. ξ_1 and ξ_2 are independent Gaussian noises.

In the first test, suppose $\beta_0 = \beta_1 = 1$ and $\beta_2 = 2$, $Z_t = \beta_0 + \beta_1 X_t + \beta_2 Y_t + \epsilon_t$. We generate series X_t and Y_t with length 10 000. Both of them share the same parameter $(d_1 = d_2)d$ ranging from -0.5 to 0.5 with the step size 0.1, and then 11 groups of series are obtained. The error term ϵ_t is set as a standard Gaussian noise, and hence the response variable Z_t has the same parameter d as the two independent variables. This case is to verify the performance of the DMA estimator under various levels of long-range dependence among series X_t, Y_t, and Z_t. The second test is designed to study how the estimator fares for long-range-dependent error terms ϵ_t. The two regression coefficients are set as the same as the first test, i.e., $Z_t = 1 + X_t + 2Y_t + \epsilon_t$. In this situation, we fix the memory parameter $d = 0.4$ for the both series X_t and Y_t. The ϵ_t is generated by an ARFIMA process with d varying from -0.5 to 0.5 with a step of 0.1. Similarly, we also get 11 groups of simulated series. Each test is run 1000 times to eliminate the noise interference and the corresponding scales vary from 10 and 100 with a logarithmic isometric step.

We show the standard deviation of all estimators varying with different parameter θ for the two experiments [see Figs. 1(a) and 1(b)]. The final results are averaged over all ds. It is clear that the central moving averaging $\theta = 0.5$ has better performance for the two tests. Furthermore, the result of the second test is much better, which contributes to the setting of error terms ϵ_t. In this regards, we take $\theta = 0.5$ in the following discussion.

Figures 2(a) and 2(b) show mean values and standard deviation of the two DMA estimators β_i^{DMA} $(i = 1$ and $2)$ for the generated series with d ranging from -0.5 to 0.5 of step size 0.1. It is clear that the two estimators locate the two given regression coefficients of 1 [Fig. 2(a)] and 2 [Fig. 2(b)] unbiasedly and are independent of the value of d. In addition, the standard deviations of both estimators decrease with the increasing memory. The narrow range of the estimators and small fluctuations show that the method is feasible. Figures 2(c) and 2(d) record similar information for the second test. The DMA estimator is again remarkably stable and unbiased for different levels of memory in the error terms. Even though variance of the estimator increases with d, which is expected due to an increasing weight of the error term in the whole dynamics of Z with the increasing memory of the error-term. For the both tests, as a comparison, we also calculate the DFA-based bivariate regression estimator [30] together with its standard deviation and show in the four subplots. Clearly, it is seen that the standard deviation of the DMA-based and DFA-based estimators possess similar trends and our DMA method is slightly superior to the DFA method.

Next, we wish to verify the antitrend performance of the proposed DMA-based regression. To this end, we employ the same bivariate regression model as the first test here. The two fractional integration parameters are set $d_1 = d_2 = 0.1$. Then we add linear trend into X_t and keep Y_t and ϵ_t unchanged. X_t with linear trend is shown in the left panel of Fig. 3. The red solid lines denote the trends: $w_t = kt$, where $t = i/100$, $i = 0, 2, \ldots, N-1$, and k denotes slope. Three slopes, namely $k = 0.01$, 0.02, and 0.03, are discussed. The OLS-based regression estimator is also calculated as a comparison. The right panel of Fig. 3 shows the result.

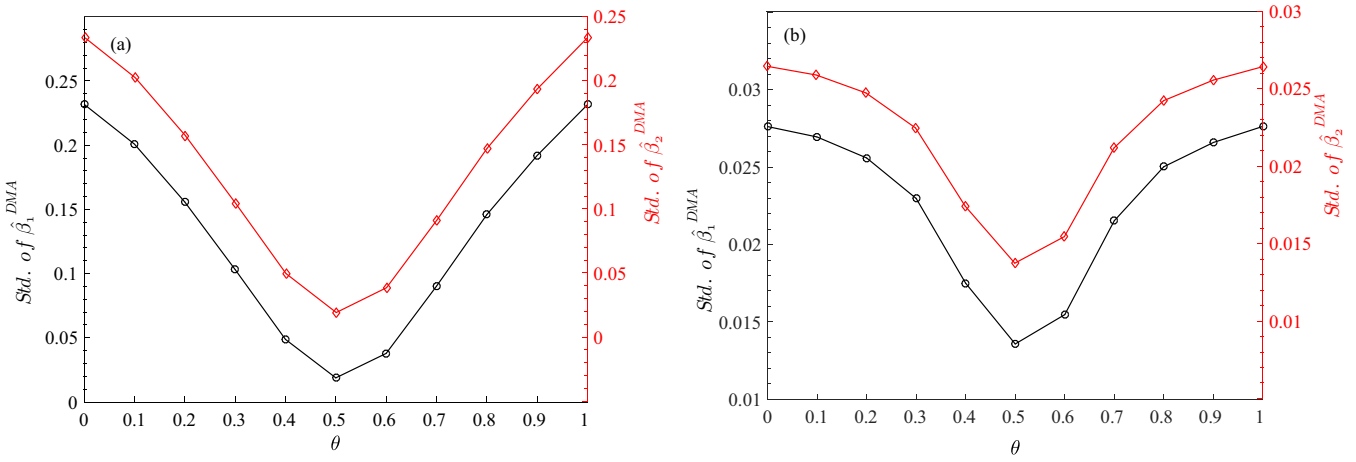

FIG. 1. Standard deviation of all estimators for $\theta \in [0, 1]$ with step size 0.1. (a) The result of the two estimated $\hat{\beta}^{\mathrm{DMA}}(s)$ for the first tests. (b) The result for the second test.

It is gratifying that $\hat{\beta}_1^{\mathrm{DMA}}(s)$ (solid lines) is stably situated nearby at 1 for available scale s regardless of trend intensity. However, the OLS-based regression model is not satisfactory. The estimated $\hat{\beta}_1$ (dotted lines) is disturbed by the trend greatly. With the increasing of trend intensity (slope), its deviation from 1 is also increasing.

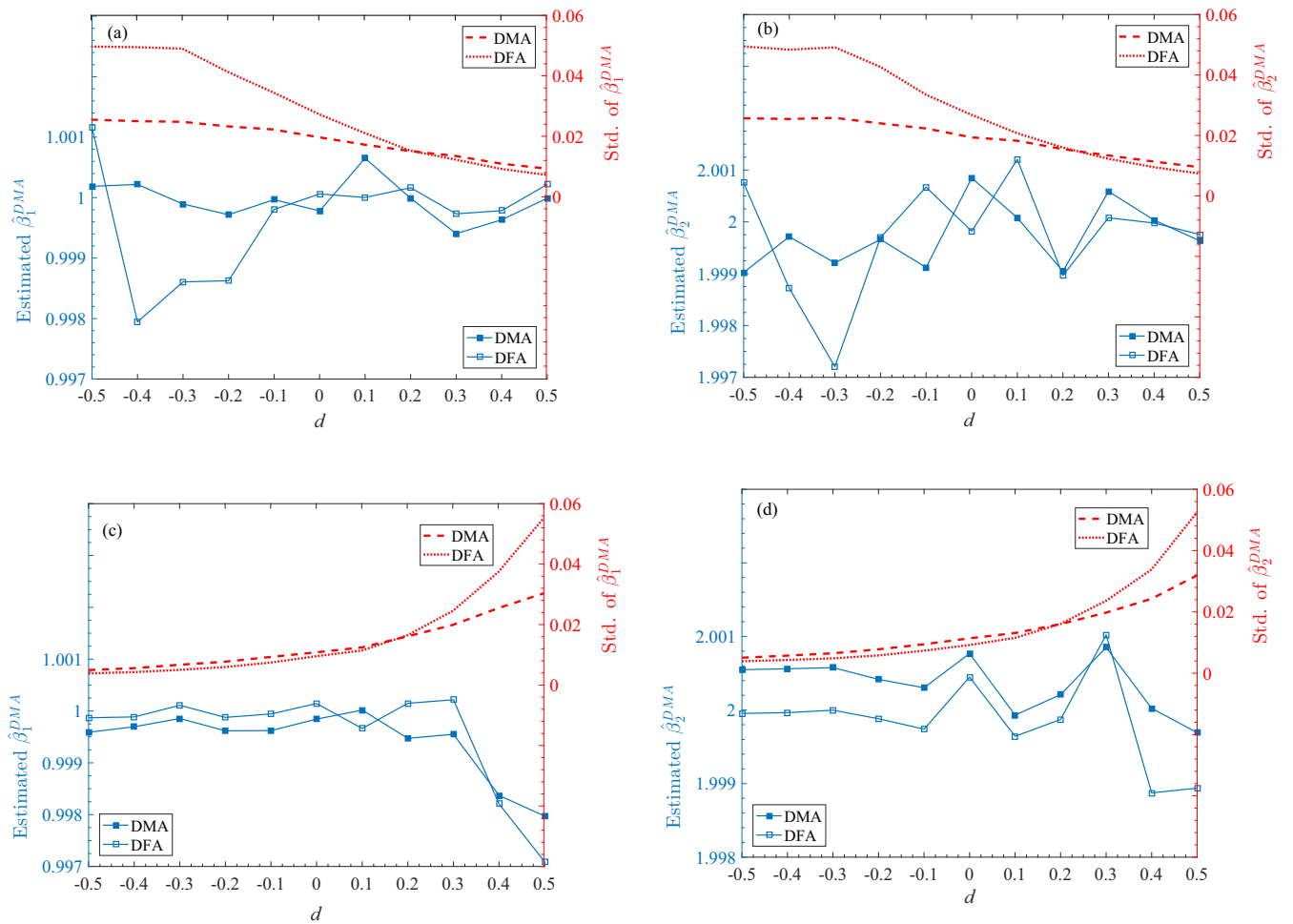

FIG. 2. Estimated two DMA regression coefficients for the two tests. [(a) and (b)] The results of the estimated $\hat{\beta}_1^{\mathrm{DMA}}(s)$ and $\hat{\beta}_2^{\mathrm{DMA}}(s)$ based on the DMA method as well as the DFA method, respectively for the first test. [(c) and (d)] Results for the second test. The two multi-scale-based estimators $\hat{\beta}_1^{\mathrm{DMA}}(s)$ and $\hat{\beta}_2^{\mathrm{DMA}}(s)$ are unbiased at 1 and 2, respectively, and their standard deviations decrease with the memory strength for the first test and increase for the second test.

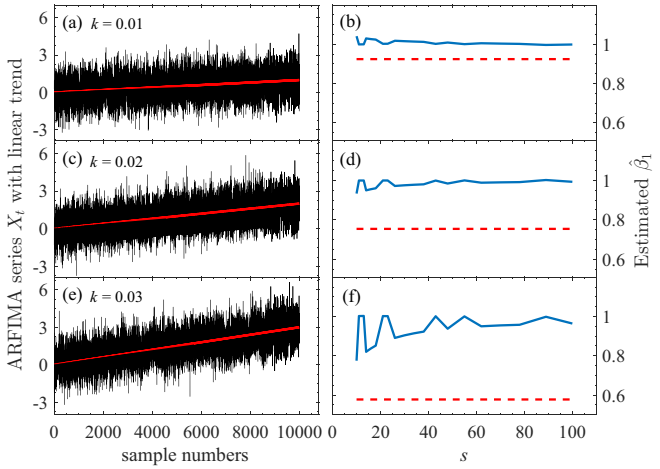

FIG. 3. Effect of linear trend on estimated regression coefficient. The left panel is X_t adding linear trend with different slope (the solid line is trend line) and the right panel is the estimated $\hat{\beta}_1$ calculated by DMA-based regression (solid line) and OSL-based regression (dotted line). Noting that the estimation of OLS-based $\hat{\beta}_1$ is seriously disturbed by the trend but the DMA-based estimator does not.

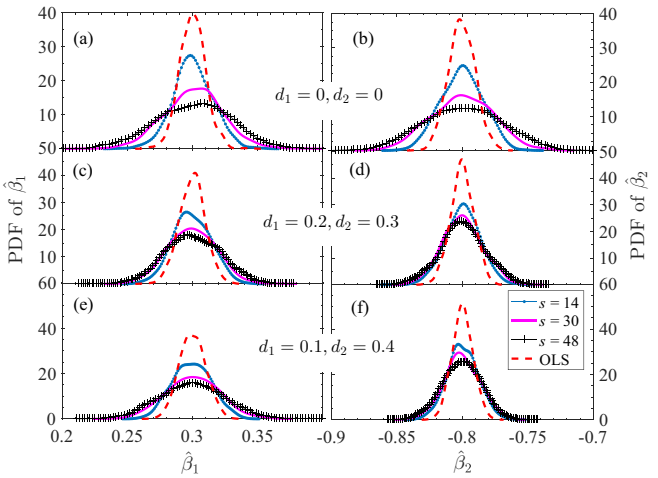

FIG. 4. PDF of regression coefficients of the DMA-based and OLS-based methods for the third test ($Z_t = 0.3X_t - 0.8Y_t + \epsilon_t$). The left panel is for $\hat{\beta}_1$ and the right panel is for $\hat{\beta}_2$. Panels (a) and (b) are for the X_t and Y_t generated by Gaussian noise ($d_1 = d_2 = 0$ in ARFIMA process). Panels (c) and (d) are for the two series generated by ARFIMA process with $d_1 = 0.2$ and $d_2 = 0.3$, respectively. Panels (e) and (f) are for $d_1 = 0.1$ and $d_2 = 0.4$. In each case, three scales s are considered for the DMA-based regression.

Finally, we discuss the distribution of the estimated regression coefficients. To do so, another bivariate regression model is considered, i.e., $\beta_0 = 0$, $\beta_1 = 0.3$, and $\beta_2 = -0.8$ for $Z_t = \beta_0 + \beta_1 X_t + \beta_2 Y_t + \epsilon_t$. Three groups of (X, Y) are generated by AFRIMA with different fractional integration parameters, namely $\{d_1 = 0, d_2 = 0\}$, $\{d_1 = 0.2, d_2 = 0.3\}$, and $\{d_1 = 0.1, d_2 = 0.4\}$. The first case means that X and Y are Gaussian white noises, and the last two cases illustrate that X and Y are power-law correlated variables, respectively. Similarly to the former tests, 1000 independent calculations are conducted for those cases. We record the PDF of the two regression coefficient estimators in Fig. 4. The left panel is for $\hat{\beta}_1$ and the right panel is for $\hat{\beta}_2$. For each group, the results for scales $s = 14$, 10, and 48 are exhibited. In addition to the DMA-based regression, we also show the PDF of the two estimators obtained from standard regression with OLS method. It is not surprising that the PDFs are a normal shape which are centered at 0.3 and -0.8, respectively, for both the DMA-based and OLS-based methods. Compared with the OLS method, the standard deviation of $\hat{\beta}_j^{\mathrm{DMA}}(s)$ is larger and increases with the increasing of scale s. Some subtle properties are unveiled for both methods. The standard deviation of $\hat{\beta}_2$ is slightly smaller than that of $\hat{\beta}_1$ due to the stronger long-term correlation of series Y (i.e., d_2 is larger than d_1). That is, the divergence between the two standard deviations of the estimated regression coefficients depends on the fractional integration parameters.

IV. APPLICATION TO FINANCIAL DATA

Many researchers have found short-term or long-term interdependence of the returns among different stock markets [33]. Especially, the linkages among Asian stock markets have become increasingly more evident in recent years [34–39]. The empirical analysis that will be carried out is to explore the dependence among stock indices of three Asian countries by the proposed DMA-based bivariate regression estimator. The Shanghai Stock Exchange Composite Index (SSEC), the Hong Kong Hang Seng Index (HSI), and NIKKEI 225 index

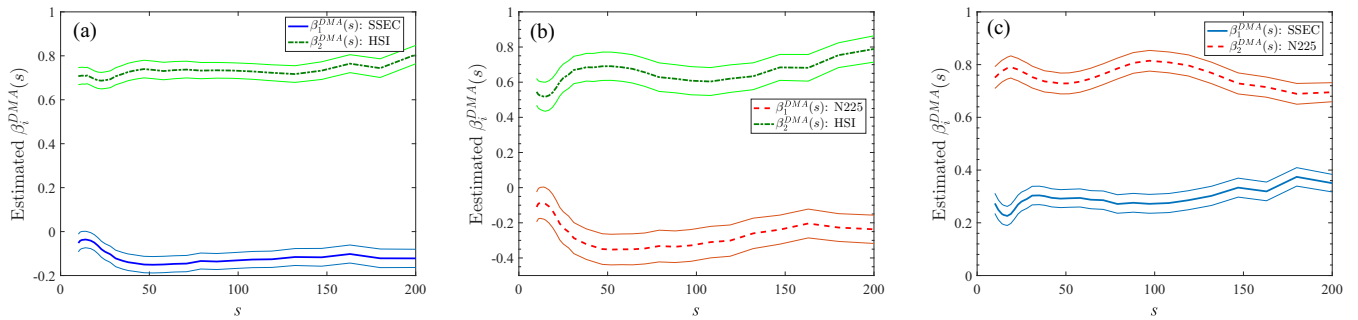

FIG. 5. Bivariate DMA regression for the three models. Light-colored zones denote 95% confidence intervals. (a) For model I. $\hat{\beta}_1^{\mathrm{DMA}}(s)$ and $\hat{\beta}_2^{\mathrm{DMA}}(s)$ are the estimated coefficient of SSEC and HSI, respectively. (b) For model II. $\hat{\beta}_1^{\mathrm{DMA}}(s)$ and $\hat{\beta}_2^{\mathrm{DMA}}(s)$ are the estimated coefficient of N225 and HSI, respectively. (c) For model III. $\hat{\beta}_1^{\mathrm{DMA}}(s)$ and $\hat{\beta}_2^{\mathrm{DMA}}(s)$ are the estimated coefficient of SSEC and N225, respectively.

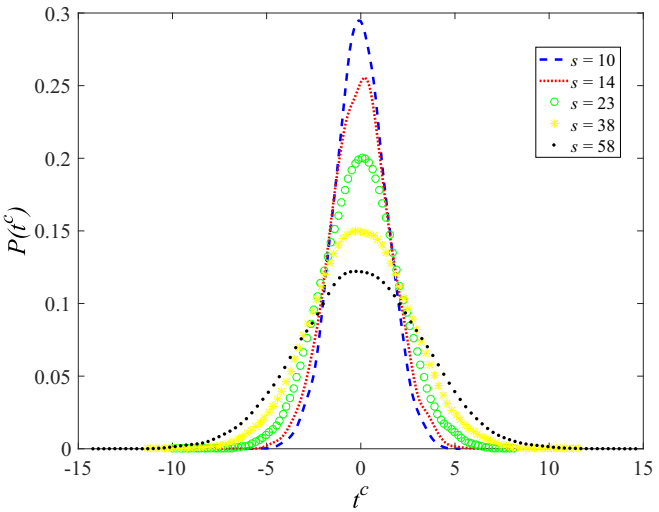

FIG. 6. PDF of critical points t statistic at different scales for the statistical test with 10 000 times of the shuffled investigated series.

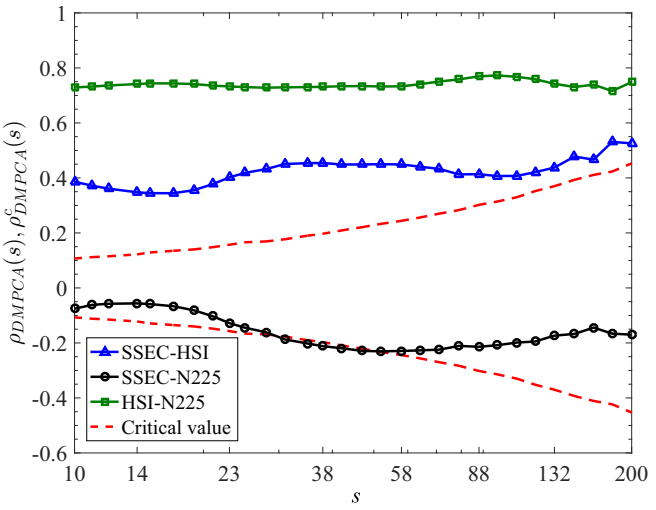

FIG. 8. Statistical test of DMPCA-based correlation coefficients among the three stock index return series. The red dotted line represents the $\rho^c_{\mathrm{DMPCA}}(s)$ with 0.01 significant level.

(N225) are the representatives of the mainland China, Hong Kong, and Japan stock markets, respectively.

This paper samples daily data from January 2007 to December 2011, which includes the global financial crisis period of 2008–2009. All these indexes are collected from the RESSET database. After the elimination of incomplete data, there are 1124 observations. Since we will use the index return instead of the raw data, the return is defined as the daily difference of the logarithmic closing prices.

A. DMA-based bivariate regression coefficients

Three bivariate models are built for SSEC, HSI, and N225, respectively. In model I, the dependent variable (Z) is the N225 series while the two independent variables are the SSEC series (X) and HSI series (Y); in model II, (Z) is the SSEC series, (X) is the N225 series, and (Y) is the HSI series; and in model III, (Z) is the HSI series and (X) and (Y) denote the SSEC and N225 series, respectively. In this section, we first show the performance of the regression coefficients at different scales in the three models.

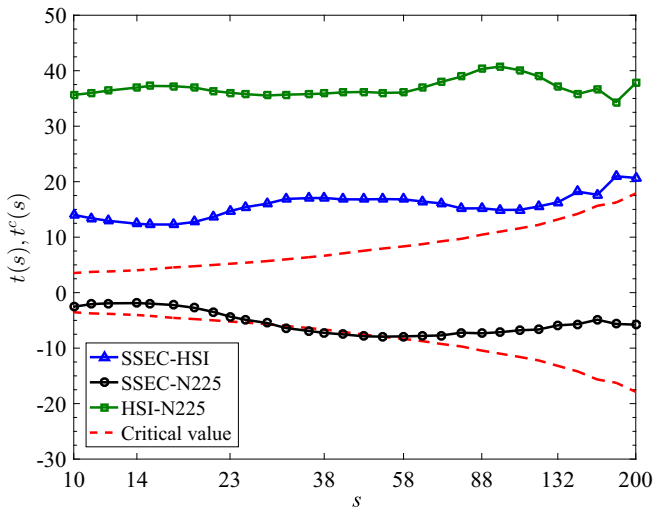

FIG. 7. The t statistical test of the estimated DMA-based bivariate regression coefficients. The red dotted line represents the $t^c(s)$ with 0.01 significant level.

Figures 5(a)–5(c) show the two regression coefficient estimators for the three models, respectively. In model I [see Fig. 5(a)], it is observed that SSEC has negative transmission on N225 across all timescales, which means an boost of SSEC is connected to a depression of N225. While the effect of HSI is positive, and the transmission of HSI to N225 is very stable across scales with the effect of between 0.6 and 0.8. This means that if the HSI increases by a single percentage point, then the N225 appreciate by between 0.6 and 0.8 percentage points. The effect (in absolute terms) of SSEC is lower compared to HSI. It implies that Japan stock market is more sensitive to the Hong Kong stock market. In model II [see Fig. 5(b)], HSI has a positive effect on SSEC, and N225 has a negative effect on SSEC for all timescales. Especially $\hat{\beta}_1^{\mathrm{DMA}}(s)$ (N225) fluctuates in $(-0.36, 0)$, while $\hat{\beta}_2^{\mathrm{DMA}}(s)$ (HSI) varies from approximately 0.5 to 0.8. It is explained that the transmission of HSI to SSEC is more strong. In model III [see Fig. 5(c)], both SSEC and N225 has positive effect on HSI; however, the effect of N225 is higher.

B. Statistical significance test of regression coefficients

Due to the size limitation, the estimated regression coefficients for finite time series are not equal 0 even if the impulse variables and the response variables have no dependence. Thus a hypothesis test for the estimated regression coefficients $\hat{\beta}_j^{\mathrm{DMA}}(j = 1, 2)$ should be carried out to ensure the significance. In standard regression analysis, the t statistic $t_j = \frac{\hat{\beta}_j - \beta_j}{\sqrt{\mathrm{var}(\beta_j)}}$ is utilized in the hypothesis test, where $t_j \sim t(N-3)$, $\hat{\beta}_j \sim N(\beta_j, \mathrm{var}(\beta_j))$.

To overcome the shortcoming of the single critical value of $t_{\alpha/2}(N-3)$ for many timescales, we follow the idea in Ref. [40] to obtain critical value for different timescale. First,

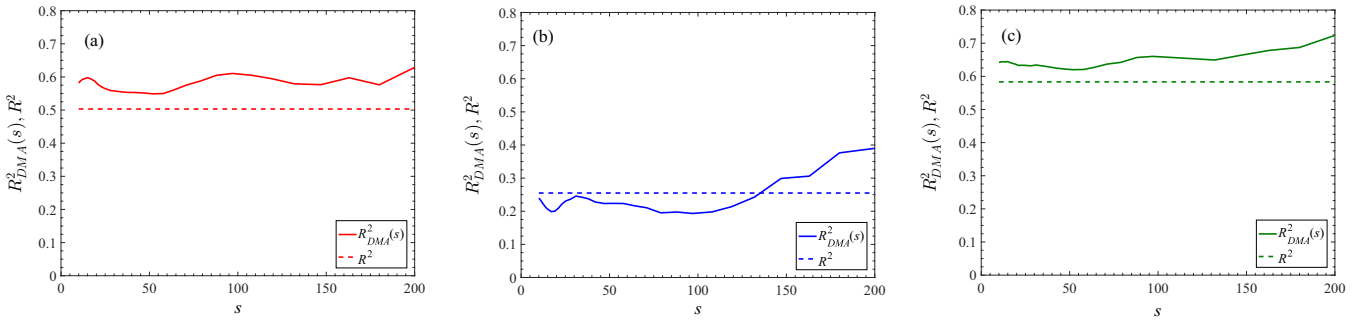

FIG. 9. Determination coefficients of bivariate DMA and standard regression model. [(a)–(c)] For models of the N225, HSI, and SSEC series, respectively. The solid line denotes $R^2_{\mathrm{DMA}}(s)$ and the dashed line denotes R^2.

by shuffling the investigated series (the three return series) and repeating the DMA-based regression coefficients' calculation for 10 000 times, let the integral of probability distribution function (PDF) from $-t^c(s)$ to $t^c(s)$ be equal to $1-\alpha$ (here we took $\alpha = 0.01$). Figure 6 shows the PDF of t statistic at different timescales with five given ss produced by the shuffled SSEC, HSI, and N225 return series 10 000 times. It can be observed that $P(t^c)$ is symmetric, and the PDF converges to a Gaussian due to the central limit theorem [41]. Moreover, the critical value increases with s's increasing. This implies that large timescale may weaken dependence between two variables. Then we calculate the practical $t_j = \frac{\hat{\beta}_j - \beta_j}{\sqrt{\mathrm{var}(\beta_j)}}$ from empirical series with the null hypothesis of $\beta_j = 0$ and compare it with the critical point t^c. If $t_j > |t^c|$, then the dependence between impulse variables and the response variables are considered statistically significant, and we reject the null hypothesis.

We obtain six $t(s)$ statistics of estimated regression coefficients $\hat{\beta}_j^{\mathrm{DMA}}(s)(j = 1, 2)$ for the three models. In fact, the $t(s)$ statistic of $\hat{\beta}_1^{\mathrm{DMA}}(s)$ (coefficient of SSEC on N225) in model I is equal the statistic of $\hat{\beta}_1^{\mathrm{DMA}}(s)$ (coefficient of N225 on SSEC) obtained in model II. Similar results are obtained for other four estimated regression coefficients. So we just consider three $t(s)$ statistics for pairs of SSEC, HSI, and N225 series. Figure 7 illustrates the $t(s)$ statistic of estimated regression coefficients and critical value $t^c(s)$.

The detrending-moving-average partial cross-correlation coefficients (DMPCA-based correlation coeffcient) $\rho_{\mathrm{DMPCA}}(s)$ for the three pairs of series (SSEC and HSI, HSI and N225, and SSEC and N225) are also calculated, which is developed to uncover the intrinsic relation for two nonstationary series at different timescales [42]. In order to test the statistical significance, we also produce a critical value for three pairs of series. Similarly, all the series are shuffled 10 000 times in the ρ_{DMPCA} calculations, and thus $\rho^c_{\mathrm{DMPCA}}(s)$ for 99% confidence level is obtained, which is also shown in Fig. 8. A similar shape of the curves can be observed in Figs. 7 and 8, which are also in agreement with the results shown in Fig. 5. The results give an interesting insight into the relationship among the three Asian stock markets. The effect of interaction is statistically significant for mainland China and Hong Kong stock market, and Hong Kong and Japan stock market for all timescales. By contrast, the influence between Hong Kong and Japan stock market is higher than that between the mainland China and Hong Kong stock markets. That is because Hong Kong and Japan have long been considered the more mature stock markets, while mainland China is a relatively new development. The significant correlation between mainland China and Hong Kong can be explained by the their close political and economic relationships. It is worth noting that, despite geographical and cultural closeness, the mainland China and Japan stock markets just exhibit significant interaction for $s \in (31, 47)$, while the dependence is rejected for other timescales. Most notably, the interaction starts about one month later and lasts just approximately 2 weeks. The result confirms that the interconnectedness between the mainland

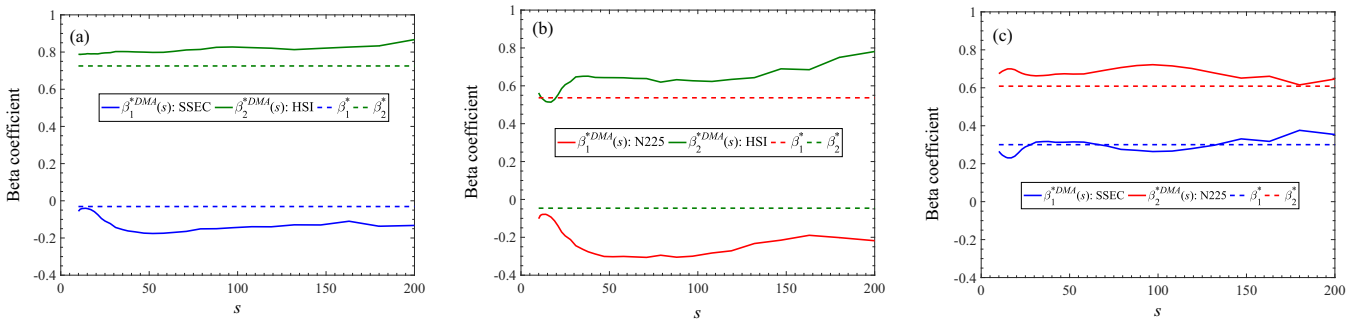

FIG. 10. β coefficients of bivariate DMA-based and the standard regression model. Panels (a)–(c) are for models of the N225, HSI, and SSEC series, respectively. The solid line denotes $\beta_j^{*\mathrm{DMA}}(s)$ and the dashed line denotes β_j^*.

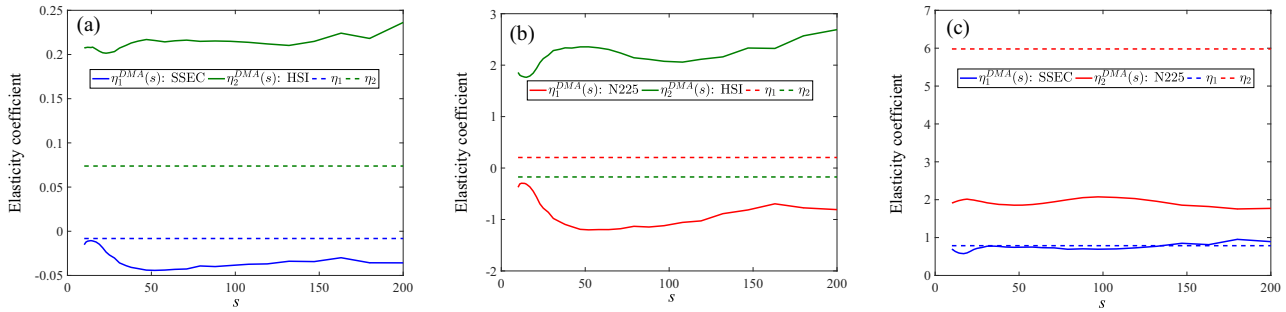

FIG. 11. Elasticity coefficients of bivariate DMA and standard regression model. Panels (a)–(c) are for models of N225, HSI, and SSEC series, respectively. The solid line denotes $\eta_j^{\mathrm{DMA}}(s)$ and the dashed line denotes η_j.

China and Japan stock markets is time dependent and they remain the least correlated pairs, although Japan is the biggest capital market among all and mainland China has a large market size and has experienced strikingly rapid growth since the late 2000s. A plausible explanation can be that the two markets are more alert to information and risk spillover from external sources, especially neighbor markets. This finding is also consistent with those reported in previous works [36,43].

C. Evaluation of DMA-based regression model

To evaluate our estimated DMA-based bivariate regression model, we plot the scale-dependent determination coefficient $R^2_{\mathrm{DMA}}(s)$, and the β coefficient $\beta^{*\mathrm{DMA}}(s)$ and the average elasticity coefficient $\eta^{\mathrm{DMA}}(s)$ in Figs. 9–11, respectively.

As seen from Fig. 9, $R^2_{\mathrm{DMA}}(s)$ is superior to the standard R^2 at most timescales. The good performance illustrates that one will gain richer information in explaining the response variable when using our DMA-based regression model. Similarly, it is observed (see Figs. 10 and 11) that β and elasticity coefficients are scale dependent. We also draw the consistent conclusion that the Hong Kong stock market has more influence than the mainland China on Japan stock markets, and the mainland China stock market is more sensitive to the fluctuation of the Hong Kong stock market, while the Japan stock market affects Hong Kong more than mainland China does.

V. CONCLUSIONS

In this work, a detrending-moving-average-based bivariate regression model is proposed. The performances of the DMA-based bivariate regression algorithms is comparable to the DFA-based method by extensive numerical experiments on pairs of time series generated from ARFIMA process. In all cases, the centered DMA algorithm performs best and the estimated regression coefficients are very close to the theoretical values. In addition, the estimated scale-dependent coefficients describe the dependence between the response variable and the two independent variables in different scales, which can provide richer information than traditional linear regression analysis.

We also applied the DMA-based bivariate regression model to the returns series of three Asian stock market indexes. The scale-dependent evaluation parameters also show that the DMA-based bivariate regression model can provide rich information across timescales. The empirical analysis shows that the Hong Kong stock market has more influence than the mainland China on Japan stock markets, and the mainland China stock market is more sensitive to the fluctuations of the Hong Kong stock market, while the Japan stock market affects Hong Kong more than mainland China does. These finding are potentially interesting for international investment and risk management to understand the transmission mechanism among the stock markets.

In conclusion, we have introduced a framework of regression analysis by merging standard regression least squares with detrending-moving-average analysis. However, there are still some issues for further study. The effect of different types of trend and filters need to be validated for different artificial signals. In addition, we will employ our method to investigate the desynchronized empirical series for detecting some possible asymmetry in the information flow [9,11] in future work.

ACKNOWLEDGMENTS

We thank the anonymous reviewers for their constructive comments and suggestions, which led to a great improvement to the presentation of this work. The authors acknowledge financial support by the National Natural Science Foundation of China (Grants No. 61603283 and No. 61973111) and Fundamental Research Funds for the Central Universities (Grants No. 2018-IB-020, No. 2019-IB-012, and No. 2020-IB-003).

[1] C. K. Peng, S. V. Buldyrev, S. Havlin, M. Simons, H. E. Stanley, and A. L. Goldberger, Phys. Rev. E **49**, 1685 (1994).

[2] C. K. Peng, S. Havlin, H. E. Stanley, and A. L. Goldberger, Chaos **5**, 82 (1995).

[3] S. V. Buldyrev, A. L. Goldberger, S. Havlin, R. N. Mantegna, M. E. Matsa, C. K. Peng, M. Simons, and H. E. Stanley, Phys. Rev. E **51**, 5084 (1995).

[4] J. W. Kantelhardt, S. A. Zschiegner, E. Koscielny-Bunde, S. Havlin, A. Bunde, and H. E. Stanley, Physica A **316**, 87 (2002).

[5] F. Wang, G. P. Liao, J. H. Li, X. C. Li, and T. J. Zhou, Physica A **392**, 5723 (2013).
[6] M. Jannesar, T. Jamali, A. Sadeghi, S. M. S. Movahed, G. Fesler, E. Meyer, B. Khoshnevisan, and G. R. Jafari, Phys. Rev. E **95**, 062802 (2017).
[7] M. Höll, K. Kiyono, and H. Kantz, Phys. Rev. E **99**, 033305 (2019).
[8] R. Gębarowski, P. Oświęcimka, M. Wątorek, and S. Drożdż, Nonlinear Dyn. **98**, 2349 (2019).
[9] M. Wątorek, S. Drożdż, P. Oświęcimka, and M. Stanuszek, Energy Econ. **81**, 874 (2019).
[10] Z.-Q. Jiang, W.-J. Xie, W.-X. Zhou, and D. Sornette, Rep. Prog. Phys. **82**, 125901 (2019).
[11] F. Wang, W. C. Zhao, and S. Jiang, Nonlinear Dyn. **99**, 1451 (2020).
[12] N. Vandewalle and M. Ausloos, Phys. Rev. E **58**, 6832 (1998).
[13] E. Alessio, A. Carbone, G. Castelli, and V. Frappietro, Eur. Phys. J. B **27**, 197 (2002).
[14] J. Alvarez-Ramirez, E. Rodriguez, and J. C. Echeverría, Physica A **354**, 199 (2005).
[15] S. Arianos and A. Carbone, Physica A **382**, 9 (2007).
[16] G. F. Gu and W. X. Zhou, Phys. Rev. E **82**, 011136 (2010).
[17] Z. Q. Jiang and W. X. Zhou, Phys. Rev. E **84**, 016106 (2011).
[18] L. Y. He and S. P. Chen, Physica A **390**, 3806 (2011).
[19] F. Wang, L. Wang, and R. B. Zou, Chaos **24**, 033127 (2014).
[20] Y. Tsujimoto, Y. Miki, S. Shimatani, and K. Kiyono, Phys. Rev. E **93**, 053304 (2016).
[21] A. Carbone and K. Kiyono, Phys. Rev. E **93**, 063309 (2016).
[22] D. Grech and Z. Mazur, Acta Phys. Pol. B **36**, 2403 (2005).
[23] L. M. Xu, P. C. Ivanov, K. Hu, Z. Chen, A. Carbone, and H. E. Stanley, Phys. Rev. E **71**, 051101 (2005).
[24] A. Bashan, R. Bartsch, J. W. Kantelhardt, and S. Havlin, Physica A **387**, 5080 (2008).
[25] Y. H. Shao, G. F. Gu, Z. Q. Jiang, W. X. Zhou, and D. Sornette, Sci. Rep. **2**, 835 (2012).
[26] L. Kristoufek, Physica A **406**, 169 (2014).
[27] L. Kristoufek, Phys. Rev. E **91**, 022802 (2015).
[28] L. Kristoufek, Acta Phys. Pol. A **129**, 908 (2016).
[29] B. Podobnik and H. E. Stanley, Phys. Rev. Lett. **100**, 084102 (2008).
[30] F. Wang, L. Wang, and Y. M. Chen, Sci. Rep. **8**, 7475 (2018).
[31] A. Carbone and G. Castelli, Proc. SPIE **5114**, 406 (2003).
[32] J. Hosking, Biometrika **68**, 165 (1981).
[33] X. Zhou, W. Zhang, and J. Zhang, Pac.-Basin Financ. J. **20**, 247 (2012).
[34] D. E. Allen, R. Amram, and M. McAleer, Math. Comput. Simul. **94**, 238 (2013).
[35] T. L. Huang and H. J. Kuo, Asia Pac. Manag. Rev. **20**, 65 (2015).
[36] R. Huo and A. D. Ahmed, Econ. Model. **61**, 260 (2017).
[37] J.-H. Schuenemann, N. Ribberink, and N. Katenka, Asia Pacific Management Review **25**, 99 (2020).
[38] Z. F. Dai, H. Zhou, F. Wen, and S. He, North Am. J. Econ. Financ. **52**, 101174 (2020).
[39] Z. F. Dai, X. D. Dong, J. Kang, and L. Y. Hong, North Am. J. Econ. Financ. **53**, 101216 (2020).
[40] B. Podobnik, Z. Q. Jiang, W. X. Zhou, and H. E. Stanley, Phys. Rev. E **84**, 066118 (2011).
[41] R. H. Shumway and D. S. Stoffer, *Time Series Analysis and Its Applications* (Springer-Verlag, New York, 2000).
[42] N. Zhang, A. Lin, and P. Yang, Physica A **542**, 122960 (2020).
[43] F. Wu, Int. Rev. Financ. Anal. **67**, 101416 (2020).